第 22 卷 增 1
2003 年 7 月
岩石力学与工程学报
Chinese Journal of Rock Mechanics and Engineering
22(增 1): 2138~2144
July, 2003

DYNAMIC BREAKAGE AND FRAGMENTATION OF BRITTLE SINGLE PARTICLE OF VARIOUS SIZES AND STRENGTH

Chau K T[1], Wu S Z[1], Wong R H C[1], Zhu W C[2], Tang C A[2], Yu T X[3]
([1]*Department of Civil and Structural Engineering, The Hong Kong Polytechnic University, Kowloon, Hong Kong, China*)
([2]*Center for Rock Instability and Seismicity Research, Northeastern University, Shenyang 110004 China*)
([3]*Department of Mechanical Engineering, The Hong Kong University of Science and Technology, Hong Kong, China*)

Abstract Breakage, comminution, crushing and fragmentation of brittle solids under dynamic impacts are an important applied mechanics and rock mechanics problem. In civil engineering applications, impact-induced-fragmentation relates to crushing of rock mass during mining process, tunneling, and aggregate production. The main objective of this paper is to outline some of our recent experimental, analytical and numerical efforts in studying the dynamic fragmentation process in brittle particle. First, an analytical solution of a solid sphere compressed dynamically between two rigid flat platens is derived analytically. Secondly, a sequence of double impact tests on spheres were conducted using an impactor Dynatup 8250 at HKUST, with both impact velocity and contact force at the impactor measured accurately. Finally, a newly developed computer program, DIFAR, is used to investigate the mechanism of dynamic fragmentation. The paper will summarize and discuss briefly all three aspects of our comprehensive approach.

Key words damage mechanics, fragmentation, dynamic impact, brittle particles
CLC number O 346.5 **Document code** A **Article ID** 1000-6915(2003)Supp.1-2138-07

1 INTRODUCTION

Breakage, comminution, crushing, fracturing and fragmentation of brittle solids under dynamic impacts are an important rock mechanics problem with academic merit as well as practical value. It relates to a wide range of phenomena and industrial processing of powders such as pharmaceuticals, chemical, fertilizers and detergents. In civil engineering applications, impact-induced-fragmentation relates to crushing of rock mass during mining process, blasting fragmentation of rock in tunneling, and aggregate production. The theory of dynamic fragmentation is relatively less developed comparing to the static counterpart, and dynamic fragmentation mechanisms remain elusive. Because of the difficulty of monitoring the fragmentation sequence inside a solid under an impact load of extremely short duration, our knowledge on dynamic fragmentation process is quite limited; thereby fragmentation is still mainly modeled by empirical approach. A comprehensive review on this problem has been given by Chau et al. (1999, 2000)[1, 2] and by Wu (2003)[3]; thus, it will not be repeated here due to page limitation. The main objective of this paper is to summarize our comprehensive approach by using analytical, experimental and numerical analyses to investigate

Received 31 March 2003.
Chau K T: Corresponding author, Male, Professor, Department of Civil and Structural Engineering, The Hong Kong Polytechnic University, Kowloon, Hong Kong, China.

fragmentation of solids.

First of all, the analytical solution of a solid sphere compressed dynamically between two rigid flat platens is considered. Secondly, a sequence of experiments on this setting are conducted using an impactor Dynatup 8250 at HKUST. Finally, a newly developed computer program, DIFAR, is used to investigate the mechanism of dynamic fragmentation.

In our experiments, brittle spheres made of plaster of two different strengths and three different sizes were compressed dynamically between two rigid platens at various impact energy levels. Fractures can be broadly classified as primary and secondary. The resulting fragments after impact can be fit into a double-log scale plot for the cumulative mass versus size (or the so-called Gates-Gaudin-Schuhmann distribution as discussed by Kelly and Spottiswood, 1982[4]). As expected, number of fragments increases with the impact energy, but surprisingly the maximum contact forces at failure remain independent of the impact energy level. The inferred specific surface energy increases with the strength but constant with the size of the spheres.

In our numerical analysis, a newly developed computer program, DIFAR (or dynamic incremental failure analysis for rocks), is used to simulate the progressive process of dynamic fracturing and fragmentations. The computer program is based on an elastic finite element analysis of solids with a loading-rate-sensitive Mohr-Coulomb criterion with a tensile cut-off. Both modulus and strength of all elements follows a Weibull distribution spatially, thus the randomness of initiation of fragmentation can be modeled. The simulated fragmentations of spheres subject to double impacts under various energies agree well with the general pattern of observations in experiments. The results of this study should provide some insight on dynamic fragmentation and a benchmark study for further research in the area.

2 THEORETICAL SOLUTION

In this section, the analytical solution for problem shown in Fig.1 is summarized. In particular, the dynamic stress distribution within an isotropic elastic solid sphere subject to a pair of suddenly-applied patch loads (either uniform or Hertz type contact stress) along a diameter is obtained using eigen-function expansion, in which the dynamic solution is decomposed into a static solution and a series of free vibration solutions. The free vibration problems are subject to an initial displacement and velocity of the sphere which is resulted from the corresponding static problem (Eringen and Suhubi, 1975[5]).

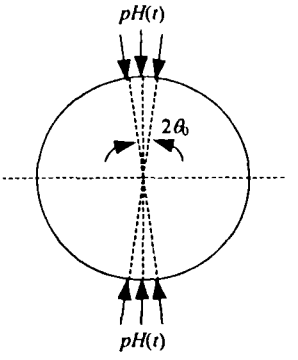

Fig.1 The theoretical model for a finite solid cylinder under the Brazilian test

2.1 Static solution

In particular, following the approach by Hiramatsu and Oka (1966[6]) for uniform contact stress applied to a sphere, the following hoop stress can be obtained:

$$\sigma_{\theta\theta}^{0}=\sum_{n=0}^{\infty}p_{2n}(\cos\theta)\left[\frac{(2n+3)\lambda-2(n-1)\mu}{4n+3}A_{2n}r^{2n}+4n\mu C_{2n}r^{2n-2}\right]+2\frac{\partial^{2}}{\partial\theta^{2}}p_{2n}(\cos\theta)\cdot\left[-\frac{(2n+3)\lambda+(2n+5)\mu}{2(2n+1)(4n+3)}A_{2n}r^{2n}+\mu C_{2n}r^{2n-2}\right] \quad (1)$$

where

$$A_{2n}=-\frac{(4n+3)(4n+1)}{[(8n^{2}+8n+3)\lambda+2(4n^{2}+2n+1)\mu]a^{2n}}\cdot[\cos\theta_{0}p_{2n}(\cos\theta_{0})-p_{2n-1}(\cos\theta_{0})]p$$

$$C_{2n}=\frac{4n(n+1)\lambda+(4n^{2}+4n-1)\mu}{2(2n-1)(2n+1)(4n+3)\mu}a^{2}A_{2n} \quad (2)$$

and

$$p=\frac{F}{2\pi a^{2}}\frac{1}{1-\cos\theta_{0}} \quad (3)$$

A more complicated solution for the case of Hertz contact stress along the loading axis has been derived, but it will not be reported here. Full details

are referred to Wu (2003)[3]. This solution also agrees with the isotropic limit of Chau and Wei (2000)[2].

2.2 Dynamic solution

The associated free vibration problem was expressed by introducing Helmholtz decomposition theorem (Eringen and Suhubi, 1975)[5] as

$$V = \nabla\Phi + \nabla\Psi \tag{4}$$

Without going into the complicated mathematical details, we only report the final solution:

$$\sigma_{\theta\theta} = \sum_{n=0}^{\infty}\sum_{m=1}^{\infty} 2\mu A_{nm}\left[H_{nm1}(r,k_{nm})p_n(\cos\theta) + H_{nm2}(r,\ k_{nm})\frac{\partial^2}{\partial\theta^2}P_n(\cos\theta)\right]\cos k_{nm}t \tag{5}$$

where

$$\left.\begin{aligned} H_{n1} &= \left\{\left[\frac{\nu}{-1+2\nu}\left(\frac{k_n}{c_1}r\right)^2 + n\right]J_{n+1/2}\left(\frac{k_n}{c_1}r\right) - \left(\frac{k_n}{c_1}r\right)J_{n+3/2}\left(\frac{k_n}{c_1}r\right) + \frac{B_n}{A_n}n(n+1)J_{n+1/2}\left(\frac{k_n}{c_2}r\right)\right\}r^{-5/2} \\ H_{n2} &= \left\{J_{n+1/2}\left(\frac{k_n}{c_1}r\right) + \frac{B_n}{A_n}\left[(n+1)J_{n+1/2}\left(\frac{k_n}{c_2}r\right) - \left(\frac{k_n}{c_2}r\right)J_{n+3/2}\left(\frac{k_n}{c_2}r\right)\right]\right\}r^{-5/2} \end{aligned}\right\} \tag{6}$$

The natural frequency of the sphere is denoted by k_n and can be calculated as (for $n = 0$):

$$\left\{n(n-1) - \frac{1-\nu}{1-2\nu}\left(\frac{k_n}{c_1}a\right)^2\right\}J_{n+1/2}\left(\frac{k_n}{c_1}a\right) + 2\frac{k_n}{c_1}aJ_{n+3/2}\left(\frac{k_n}{c_1}a\right) = 0 \quad (n = 1,\ 3,\ 5,\ \cdots) \tag{7}$$

$$2n(n+1)\left[(n-1)J_{n+1/2}\left(\frac{k_n}{c_2}a\right) - \frac{k_n}{c_2}aJ_{n+3/2}\left(\frac{k_n}{c_2}a\right)\right]\cdot\left[(n-1)J_{n+1/2}\left(\frac{k_n}{c_1}a\right) - \frac{k_n}{c_1}aJ_{n+3/2}\left(\frac{k_n}{c_1}a\right)\right] + \left\{\left[n(n-1) - \frac{1-\nu}{1-2\nu}\left(\frac{k_n}{c_1}a\right)^2\right]J_{n+1/2}\left(\frac{k_n}{c_1}a\right) + 2\frac{k_n}{c_1}aJ_{n+3/2}\left(\frac{k_n}{c_1}a\right)\right\}\left[\left(-2n^2+2+\frac{k_n^2}{c_2^2}a^2\right)J_{n+1/2}\left(\frac{k_n}{c_2}a\right) - 2\left(\frac{k_n}{c_2}\right)aJ_{n+3/2}\left(\frac{k_n}{c_2}a\right)\right] = 0 \tag{8}$$

The unknown constants A_{nm} have to be found by using the initial condition imposed by the static solution. That is

$$V(x,\ 0) = U(x) \tag{9}$$

where $U(x)$ is the displacement solution of the static problem considered in Section 2.1. The final solution is

$$A_{(2n+1)m} = 0$$

$$A_{2nm} = \left[-\frac{n\lambda + (n-1)\mu}{(4n+3)\mu}A_{2n}I_1 + 2nC_{2n}I_2 + \frac{(2n+3)\lambda + (2n+5)\mu}{(4n+3)\mu}nA_{2n}I_3 - 2n(2n+1)C_{2n}I_4\right]\Big/I_7 \tag{10}$$

where

$$I_1 = \int_0^a r^{2n+3}u_{2nm}\mathrm{d}r \quad I_2 = \int_0^a r^{2n+1}u_{2nm}\mathrm{d}r$$

$$I_3 = \int_0^a r^{2n+3}v_{2nm}\mathrm{d}r \quad I_4 = \int_0^a r^{2n+1}v_{2nm}\mathrm{d}r$$

$$I_5 = \int_0^a r^2u_{2nm}^2\mathrm{d}r \quad I_6 = \int_0^a r^2v_{2nm}^2\mathrm{d}r$$

$$I_7 = I_5 + 2n(2n+1)I_6$$

2.3 Impact dynamic solution

Thus the final solution of the double impact problem can be obtained as

$$\sigma_{\theta\theta}^{\mathrm{d}} = \sigma_{\theta\theta}^{0} - \sigma_{\theta\theta} \tag{11}$$

where σ^0 and σ^{d} are the static stress given in Sect. 2.1 and the dynamic stress given in Sect. 2.2, respectively.

The analytical solution form given in equation (5) is in terms of a double infinite series involving Legendre polynomials and spherical Bessel function. For the special case that the patch converges to a pair of applied point loads, our solution is comparable to those obtained by Jingu and Nezu (1985)[7], when transmission of waves through the two rigid platens is allowed for the long term solutions converge to the static solution given by Hiramatsu and Oka (1966)[6] and to the isotropic limit of Chau and Wei (2000)[2] solution for cases of uniform and Hertz contact loads, respectively.

To fully visualize the prediction of this solution, Fig.2 shows the major principal stress (or the most compressive stress) in a quadrant of the sphere due to

symmetry. The time of the plot is at a/c_1 where a is the radius of the sphere and c_1 is the compressional wave speed of the solid sphere. That is, the plot is for the time when the compression wave reaches the center of the sphere.

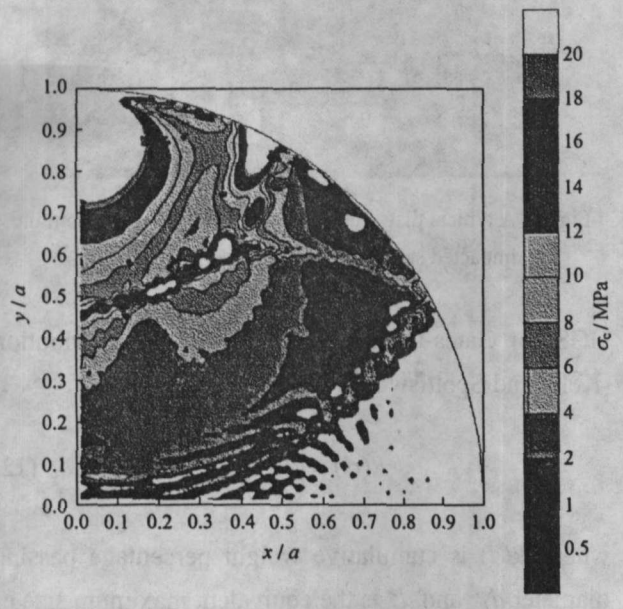

Fig.2 Theoretical contour plot for the maximum compressive stress at time a/c_1 induced by double impact test(stress normalized with respect to $F/\pi a^2$)

Similarly, Figs.3 and 4 plot the minimum principal stress (or the most tensile stress) and the shear stress in the same quadrant of the sphere. It is clear from Figs. 2～4 that the locations of the most compressive, tensile and shear zones coincides in these

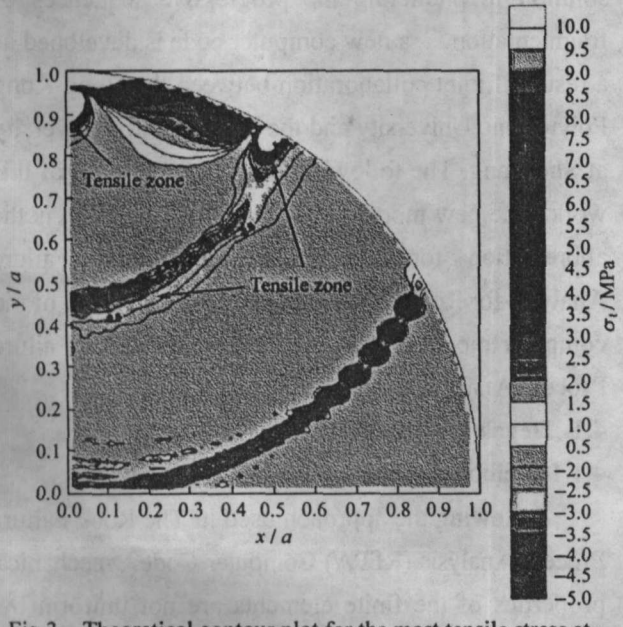

Fig.3 Theoretical contour plot for the most tensile stress at time a/c_1 induced by double impact test(stress normalized with respect to $F/\pi a^2$)

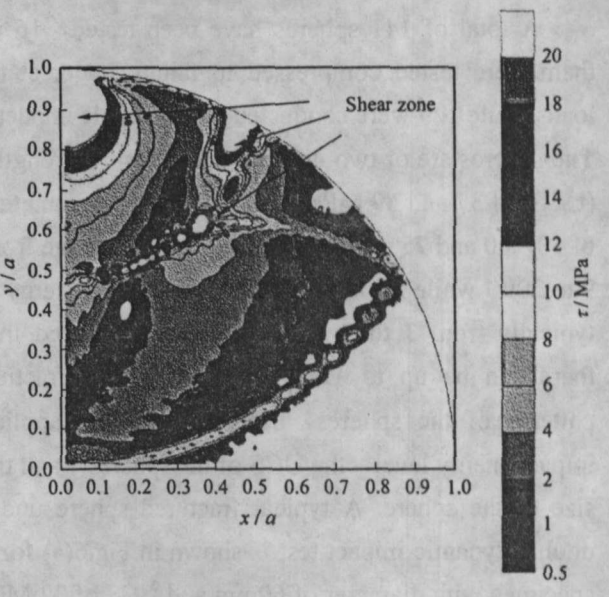

Fig.4 Theoretical contour plot for the maximum shear stress at time a/c_1 induced by double impact test(stress normalized with respect to $F/\pi a^2$)

diagrams. Thus, these plots clearly indicate that certain regions are more conducive to fracture initiation than others at certain time. Wu (2003)[3] have more thoroughly analyzed the region of highest stress concentrations at different time, but the details will not be given here.

3 EXPERIEMNTS

As part of our comprehensive studies on the fragmentation of a single particle, some double dynamic impact tests very similar to the one considered in Section 2 have been conducted at HKUST using the Dynatup 8250 impactor (shown in Fig.5), using which the impact energy, impact velocity and impact force can be accurately measured in the order of 0.01 ms.

Fig.5 The Dynatup 8250 impactor at HKUST

A total of 141 spheres have been tested, 16 of them were tested compressed to failure under static loads while 125 were conducted under double impacts. The spheres are of two uniaxial compressive strengths (UCS) of 37 and 59 MPa and three different diameters of 50, 60 and 75 mm. The impact energies range from 9 to 209 J while for the static test the applied energy is typically from 3 to 9 J. It was also discovered that there can be up to 12 different failure or fracture patterns of the spheres, depending on the applied impact energy level, the UCS of the spheres, and the size of the sphere. A typical fractured sphere under double dynamic impact test is shown in Fig.6(a) for a specimen with diameter of 60mm and UCS of 37 MPa subject to an impact of 132 J; and a sketch showing the internal fractured sections of a typical specimen is shown in Fig.6(b). The calculated specific surface energy is from about 0.01 to 0.027 J/mm^2. The full details of these experiments are referred to Wu (2003)[3].

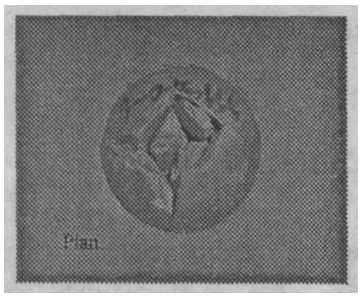

(a) A specimen with diameter of 60 mm and UCS of 37 MPa subject to an impact of 132 J

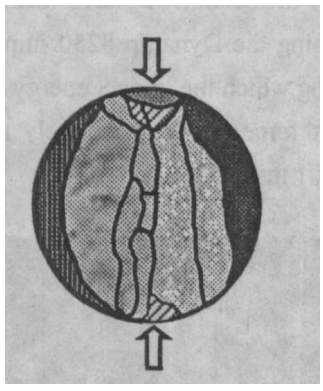

(b) A sketch showing internal fractured sections of a typical specimen

Fig.6 A typical fractured sphere under double dynamic impact test

It was also discovered that the fragments (e.g. see Fig.7) of the fractured spheres can be fit into a so-called

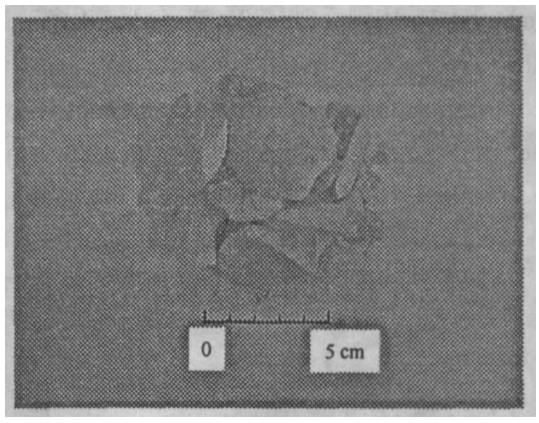

Fig.7 A typical distribution of fragments resulted from the impacted sphere

GGS (or Gates-Gaudin-Schuhmann) size distribution (Kelly and Spottiswood, 1982)[4]:

$$R(d)=\left(\frac{d}{d^*}\right)^n \tag{12}$$

where $R(d)$ is cumulative weight percentage passing diameter d, and d^* is the equivalent maximum size of fragments. We found that typically for the plaster spheres under double impact, the n value ranges from about 0.88 to 1.21, which is slightly smaller than the results for real rocks (Shockey et al., 1974)[8].

4 NUMERICAL SIMULATIONS

In view of the limitation of the theoretical solution in predicting the progressive sequences of fragmentation, a new computer code is developed as a result of joint collaboration between the Hong Kong Polytechnic University and the Northeastern University at Shenyang. The following is a brief summary of this work. The new model is called DIFAR, which is the abbreviation for " Dynamic Incremental Failure Analysis for Rock"and is the dynamic extension of the computer model RFPA, short form for Rock Failure Process Analysis (Tang 1998)[9].

4.1 Development of DIFAR

4.1.1 Weibull distribution

Following the approach used in The Rock Failure Process Analysis (RFPA) Computer Code, mechanical properties of the finite elements are not uniform but conform to the Weibull distribution. More specifically, the probability density function $f(u)$ of an element

having a value of u is

$$f(u)=\frac{m}{u_0}\left(\frac{u}{u_0}\right)^{m-1}\exp\left(-\frac{u}{u_0}\right)^{m} \tag{13}$$

where u is the considered parameter of each element (such as strength or elastic modulus), and the average of it among all elements is denoted by u_0. A key parameter in this Weibull distribution is m, which defines the shape of the distribution function such that a larger m implies a more homogeneous material while a smaller m indicates a more heterogeneous material.

4.1.2 Elastic damage approach

In order to simulate progressive damages in the finite element model, an element-level damage criteria is assumed. As for most geomaterials, the Mohr-Coulomb failure criterion is assumed here:

$$\sigma_1-\frac{1+\sin\varphi}{1-\sin\varphi}\sigma_3\geqslant f_{c0} \tag{14}$$

where σ_1 and σ_3 are the major (or most compressive) and the minor (or most tensile) principal stresses, f_{c0} is the compressive strength, and φ is the frictional angle of the Mohr-Coulomb failure criterion. Once the damage criteria (14) is satisfied at the element level, the elastic modulus of the element will be reduced to a damage level as:

$$E=(1-\omega)E_0 \tag{15}$$

where

$$\omega=\begin{cases}0 & \varepsilon_1<\varepsilon_{c0}\\ 1-\dfrac{\lambda\varepsilon_{c0}}{\varepsilon_1} & \varepsilon_1\geqslant\varepsilon_{c0}\end{cases} \tag{16}$$

$$\varepsilon_{c0}=\frac{1}{E_0}\left[f_{c0}+\frac{1+\sin\varphi}{1-\sin\varphi}\sigma_3-\nu(\sigma_1+\sigma_2)\right] \tag{17}$$

In these formulas, σ_2 is the intermediate principal stress, ε_1 is the current strain value, ω represents the damage variable, λ is a residual strength coefficient, and ν is the Poisson's ratio of the solid. Physically, once an element is damaged, it cannot be healed. Thus, the damage process in our model is irreversible. In addition, for solids under dynamic loading it is normally observed that the strength is strain-rate dependent. In this study, the following elation between dynamic uniaxial compressive strength and loading rate is assumed as

$$\sigma_{cd}=A\lg(\dot{\sigma}_{cd}/\dot{\sigma}_c)+\sigma_c \tag{18}$$

where σ_{cd} is the dynamic uniaxial compressive strength (MPa), $\dot{\sigma}_{cd}$ is the dynamic loading rate (MPa/s), and $\dot{\sigma}_c$ is the quasi-brittle loading rate (approximately 5×10^{-2} MPa/s), σ_c is the uniaxial compressive strength at the quasi-static loading rate and A is a parameter depending on the material. This kind of semi-log relationship had been used by Grady and Kipp (1979)[10] for rocks and by Tedesco et al. (1991)[11] for concrete.

4.2 Numerical simulation of fragmentation

To illustrate the progressive failure, Fig.8 shows the progressive failure of a solid sphere of diameter 60 mm and UCS of 153 MPa subject to a double impact test of energy of 20 J. The process of fragmentation can clearly be seen in Fig.8. More numerical simulations for other conditions are referred to Wu (2003)[3].

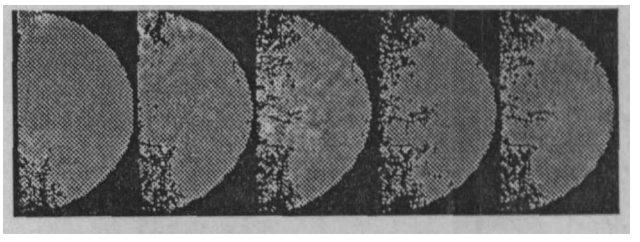

Fig.8 The mechanism of progressive failure in a solid sphere of 60 mm diameter subject to 20 J of impact energy

5 CONCLUSION

In this paper, a very comprehensive approach to investigate the dynamic breakage and fragmentation of solid particles of spherical shape is presented. It includes the use of analytical, experimental as well as numerical studies. Although there are much remains to be done, the present study provides a framework for future analysis for this complicated problem of dynamic fragmentation, which is an extremely important phenomenon in mining and tunneling problems.

Acknowledgements The work described in this paper was partially supported by a grant from the Research Grants Council of the Hong Kong Special Administrative Region, China (Project No. PolyU 5044/99E) and partially by a research studentship to

Mr. Wu S Z.

REFERENCES

1 Chau K T, Wei X X. Spherically isotropic, elastic spheres subject to diametral point load strength test[J]. International Journal of Solids and Structures, 1999, 36(29): 4 473～4 496

2 Chau K T, Wei X X, Wong R H C, et al. Fragmentation of brittle spheres under static and dynamic compressions: experiments and analyses[J]. Mechanics of Materials: An International Journal, 2000, 32(9): 543～554

3 Wu S Z. Theoretical and experimental studies on dynamic impact on brittle solids[PhD Thesis][D]. Hong Kong: The Hong Kong Polytechnic University, 2003

4 Kelly E G, Spottiswood D J. Introduction to Mineral Processing[M]. New York: Johns Wiley & Sons Inc., 1982

5 Eringen A C, Suhubi E S. Elastodynamics (I and II)[M]. New York: Academic Press, 1975

6 Hiramatsu Y, Oka Y. Determination of the tensile strength of rock by a compression test of as irregular test piece[J]. International Journal of Rock Mechanics and Mining Science, 1966, (3): 89～99

7 Jingu T, Nezu K. Transient stress in an elastic sphere under diametrical concentrated impact loads[J]. Bulletin JSME, 1985, 28(245): 2 553～2 561

8 Shockey D A, Curran D R, Seaman L, et al. Fragmentation of rock under dynamic loads[J]. International Journal of Rock Mechanics and Mining Sciences, 1974, (11): 303～317

9 Tang C A. A new approach to numerical method of modeling geological processes and rock engineering problems[J]. Engineering Geology, 1998, 49: 207～214

10 Grady D E, Kipp M E. The micromechanics of impact fracture of rock[J]. Int. J. Rock Mech. Min. Sci., 1979, 16(5): 293～302

11 Tedesco J W, Ross C A, McGill P B, et al. Numerical analysis of high strain rate concrete direct tension tests[J]. Computers & Structures, 1991, 40(2): 313～327